First light of the High Contrast Integral Field Spectrograph (HCIFS)

Christian Delacroix[a], He Sun[a], Michael Galvin[a], Mary Anne Limbach[c], Tyler Groff[b], Maxime Rizzo[b], Matthew Grossman[a], Katherine Mumm[a], N. Jeremy Kasdin[a]

[a]Mechanical & Aerospace Engineering, Princeton University, Princeton, NJ 08540;
[b]NASA Goddard Space Flight Center, Greenbelt, MD 20771;
[c]Exoplanet Consulting, College Station, TX 77845SPIE2018.

ABSTRACT

Future space-based observatories such as WFIRST will be equipped with high contrast imaging instruments designed to study extrasolar planets and disks in the absence of atmospheric perturbations. One of the most efficient techniques to achieve this goal is the combination of wavefront control and broadband coronagraphy. Being able to achieve a high contrast over a wide spectral bandwidth allows us to characterize the chemical composition of exoplanet atmospheres using an integral field spectrograph (IFS). In this paper, we report on the development of such an IFS for the High Contrast Imaging Lab (HCIL) at Princeton University, downstream of a Shaped Pupil coronagraph. Our final lenslet-based design calls for the light in an 18% band around 660 nm to be dispersed with a spectral resolution of 50. We also present our new laboratory control software written in Python, allowing the import of open-source packages such as CRISPY to ultimately reconstruct 3D datacubes from IFS spatio-spectral science images. Finally, we show and discuss our preliminary first light results, reaching a contrast of ~10^{-5} using in-house focal-plane wavefront control and estimation algorithms with two deformable mirrors.

Keywords: exoplanet, direct imaging, integral field spectrograph, coronagraph, wavefront estimation

1. INTRODUCTION

One of the most exciting challenges in exoplanet science is to take pictures of planets in the habitable zones of nearby low mass stars and look for signs of life in their atmospheric composition. Recent instruments[1] installed on ground-based observatories are limited to contrast levels of 10^{-5}–10^{-6}, mainly due to stability challenges and atmospheric perturbations. Future space observatories such as WFIRST are expected to achieve better contrasts. They will play a major role in characterizing Earthlike planets, as they will be equipped with Integral Field Spectrographs (IFS)[2]. An IFS disperses the light in the entire field of view to extract spectra from potential companion signals without prior knowledge of their position. WFIRST coronagraph instrument will feature a lenslet array-based IFS operating in 3 spectral bands of $\Delta\lambda/\lambda$ = 18% between 600 and 970 nm. In addition to obtaining planet atmospheric composition, broadband operations help reach the desired contrasts in the so-called dark holes faster than in narrow band, since both the spatial and spectral dependence of the speckle field are measured at once.[3]

In this paper, we report on the recent development of an IFS for the High Contrast Imaging Lab (HCIL) at Princeton University. The main goal of our IFS is to demonstrate closed-loop broadband wavefront control, and to develop new IFS-based wavefront estimation and control algorithms[4] and system identification techniques[5]. In Section 2, we give a description of the HCIL and its current Focal Plane Wavefront Control (FPWC) performance in monochromatic light. In Section 3, we present the optical design of the High Contrast Integral Field Spectrograph (HCIFS) and the ongoing development of our dedicated control software in Python language. Finally, we present our preliminary results with first light and first spectra, and we conclude with a discussion on future works.
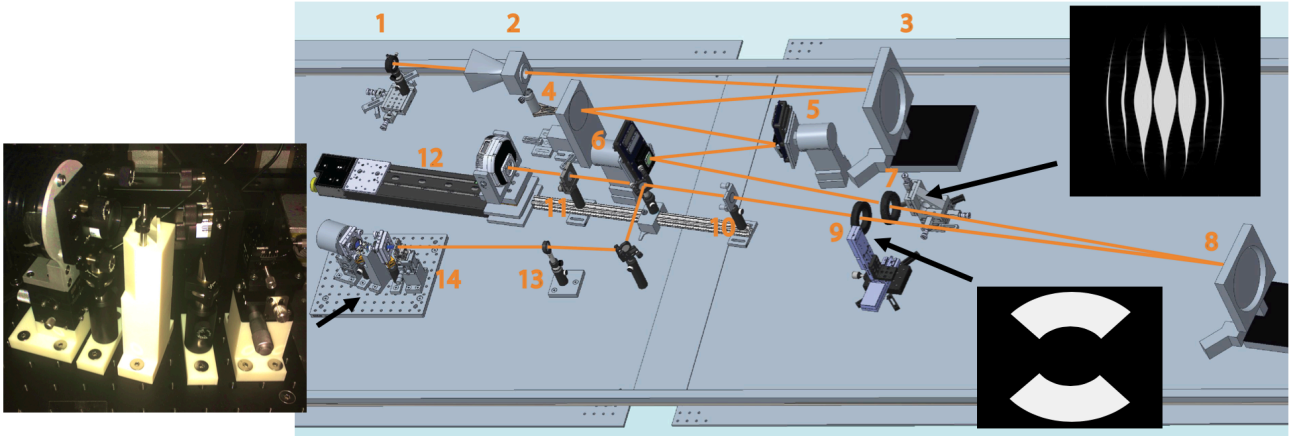
Figure 1. The HCIL current layout including the following devices: 1/ laser (red or white light), 2/ baffle, 3/ off-axis parabola, 4/ fold mirror, 5-6/ Boston Micromachine 2xkilo DMs, 7/ shaped pupil, 8/ off-axis parabola, 9/ bowtie focal plane mask, 10-11-13/ lenses, 12/ Imaging mode camera, 14/ Spectroscopy mode camera, with a photo of the Integral Field Spectrograph (IFS) on the left side.

2. THE HIGH CONTRAST IMAGING LABORATORY (HCIL)

2.1 Laboratory description

This work was conducted at the Princeton University High Contrast Imaging Laboratory (HCIL), designed to demonstrate cutting-edge technologies for exoplanet direct imaging and characterization from space-based platforms. Over the last 15 years, various shaped pupil coronagraphs and model-based wavefront control and estimation techniques have been developed and validated in the HCIL[6–15]. The testbed is located in a 900 sq. ft. clean room with temperature and humidity control. It is equipped with vibration isolation and a clean air system designed for optical research. The latest on-going developments include the addition of low-order wavefront sensing (LOWFS), and an integral field spectrograph (IFS) as presented in this paper. Fig. 1 illustrates the HCIL current layout, which can be divided into 4 sections:

1. **Star-planet simulator:** A star (and optionally a planet) is simulated with a monochromatic red laser, or polychromatic supercontinuum white light for broadband control. The collimated beam is obtained by combining a baffle and an off-axis parabola.

2. **Adaptive optics:** The light reflects off two deformable mirrors (DMs) in series, which utilize phase perturbations in the electric field in order to correct for wavefront aberrations. The DMs in use are Boston Micromachine kilo-DMs, each with 952 active actuators.

3. **Coronagraph:** After the DMs, the light passes through a ripple shaped pupil (SP), which modifies the focal plane diffraction pattern. Instead of an Airy pattern, the point spread function now has the shape of a bowtie. Most of the starlight is blocked by a bowtie focal plane mask (FPM). The two regions not blocked by the FPM are called dark holes. That is where the star companions (exoplanets) can be imaged, or even characterized with an IFS.

4. **Science instruments:** The lab currently operates in two modes. The imaging mode is equipped with a QSI-RS-6.1s camera. The spectroscopy mode uses the SXVR-H9 camera recently installed in the IFS for broadband operation, as described in the next section.

A more detailed description of the HCIL is also available on the website of the High Contrast Testbed Community at https://sites.google.com/view/highcontrastlabs/testbeds/hcil.
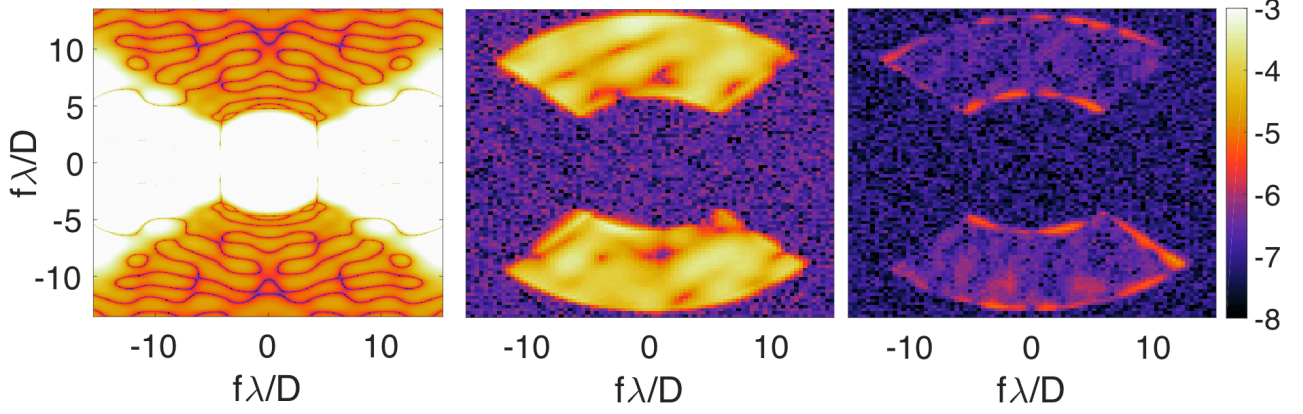
Figure 2. Normalized intensity of focal plane coronagraphic images using a ripple shaped pupil. The monochromatic source operates at a wavelength $\lambda = 632$ nm. Left: a simulation of the bowtie shaped diffraction pattern, a contrast level of 10^{-4}–10^{-5} in the dark holes. Middle: a laboratory experiment with the bowtie focal plane mask aligned on-axis, and without any FPWC. Right: the same configuration with the addition of FPWC, improving the contrast by 2 orders of magnitude.

2.2 FPWC in monochromatic light

The shaped pupil[6] coronagraph currently in use at HCIL is an optimized ripple-shaped multi-pupil as shown in Fig. 1. In theory, such a mask reduces the intensity of an on-axis source in two regions of the image plane, called dark holes. The relative intensity obtained in the dark holes is close to 10^{-5} as shown in Fig. 2, which is far from the 10^{-10} contrast required to observe Earth-like planets. Our FPWC system is used to account for wavefront aberrations using the two DMs. In the ideal case of a perfectly well known focal-plane electric field, simulations show that FPWC allows the contrast delivered by the shaped pupil coronagraph to be increased to and maintained at $\sim 10^{-11}$ in the dark holes[4]. In practice, the addition of Gaussian and Poisson noises degrade the FPWC performance to a level of $\sim 10^{-8}$.

The principle of FPWC is as follows. For each control iteration, a wavefront estimator is employed to convert the intensities received at the camera into a model of the electric field. The simplest way to do this is to use a batch process estimator (BPE). Two images are taken using positive and negative probes. The two images, for the $k-th$ iteration and the $j-th$ pixel, are

$$x_{k,j}^{\pm} = x_{k,j-1} \pm G_j u_p,$$

where $\pm u_p$ are the commands used to generate the images and G is the control effect matrix.

The intensity of the electric field, $I_{k,j}$, and the difference between the positive and negative intensities, $\Delta I_{k,j}$ are then given by

$$I_{k,j}^{\pm} = x_{k,j}^{\pm T} x_{k,j}^{\pm}$$

$$\Delta I_{k,j} = I_{k,j}^{+} - I_{k,j}^{-} = 4 u_p^T G_j^T x_{k,j}$$

The process is repeated with m pairs of opposite commands so that

$$z_{k,j} = \begin{bmatrix} \Delta I_{k,j}^1 \\ \vdots \\ \Delta I_{k,j}^m \end{bmatrix} = 4 \begin{bmatrix} u_{p,1}^T G_j^T \\ \vdots \\ u_{p,m}^T G_j^T \end{bmatrix} x_{k,j,} = H_{k,j} x_{k,j} \ .$$

Using a least-square fit creates the BPE equation, where $\hat{x}_{k,j}$ is the estimated electric field[12]

$$\hat{x}_{k,j} = (H_{k,j}^T H_{k,j})^{-1} H_{k,j}^T z_{k,j}.$$

Once the electric field is estimated, an electric field conjugation (EFC) is used as the controller to develop DM commands. The commands should aim to minimize the energy, I_k, in the target dark areas, which yields an equation for commands, u_k

$$u_k = -(G^T G)^{-1} G^T x_{k-1}.$$

This equation, however, is unstable because it creates commands that are too large. To account for this, the EFC uses a Tikhonov regularization term, α_k, so the problem becomes

$$\min x_k^T x_k + \alpha_k u_k^T u_k,$$

the solution of which is

$$u_k = -(G^T G + \alpha_k \mathbb{I})^{-1} G^T x_{k-1},$$

where $\mathbb{I}$ is the identity matrix. This is similar to the original formula, with a damping term.[15]

The generated commands are then passed to the DMs, new images are taken, and the BPE and EFC are repeated for a given number of iterations. This process has been able to reach a contrast level of 2×10^{-7} after about 20 iterations as shown in Fig. 3.
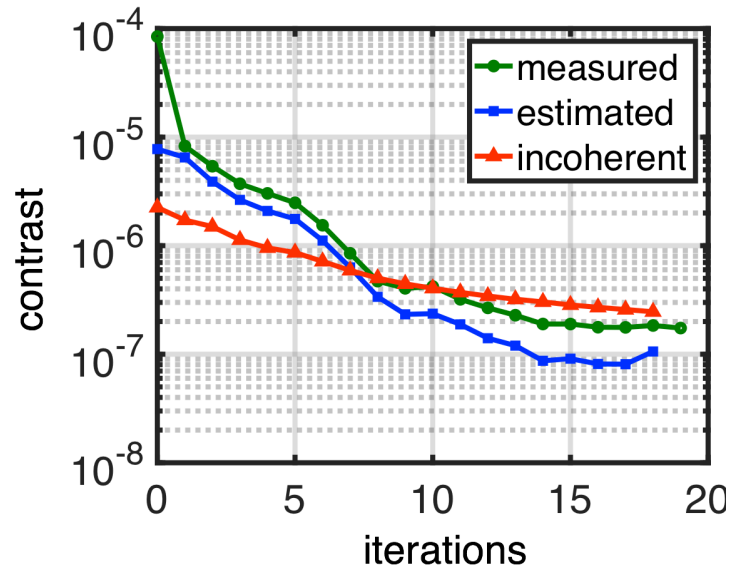
Figure 3. Contrast curve of a FPWC experiment in the HCIL using 2 deformable mirrors, batch process estimation and electric field conjugation.

It is worth noting that the estimated contrast is generally up to one order of magnitude better than the measured contrast. Our models predict an improved level of contrast that we are not able to achieve. In other words, the HCIL does not perform as well as it theoretically could. This is explained by incoherent sources of light in the lab. We have investigated multiple causes of this limitation, but we have not been able to eliminate it completely. Future efforts in that direction include:

- a better isolation from unwanted reflections of light inside the lab (i.e., taping reflective surfaces, using black paint);

- the acquisition of a better performing camera with increased sensitivity (possibly a photon counting EMCCD), to lower the noise limit and allow longer integration times with reduced laser intensity;

- a cleaner Star simulator featuring a spatial filter with a 5 μm pinhole, which implies replacing the current first parabola (1500 mm focal) with a faster one to collect more light from the spatial filter.

3. PRELIMINARY RESULTS WITH THE HCIFS

## 3.1 Building an integral field spectrograph

The optical design of the High Contrast Integral Field Spectrograph (HCIFS) was carried out in collaboration with Exoplanet Consulting (M.A. Limbach), who performed Zemax optical simulations to calculate the optimal design parameters, and preselected optics corresponding to tolerancing specifications. The IFS consists of 3 parts in series: (i) the pre-lenslet optics, (ii) the lenslet array, and (iii) the spectrograph optics.

Pre-lenslet optics

As illustrated in Fig. 1, the IFS uses 2 flat mirrors to pickoff a collimated beam of 1.5 mm in diameter. The beam passes through a 400 mm focusing lens, which gives a F/260 system.

Lenslet array

We use a microlens (or lenslet) array at the focus of our slow F/# beam to Nyquist sample the primary image and create an array of small point spread functions (or PSFlets) in the sparse image. Our design goal is to have 2 lenslets per λ/D, which corresponds to 171.4 µm on the camera and a field of view of 26×19 λ/D. This determines the length and spacing of each spatial element (spaxel), as illustrated in Fig. 4.
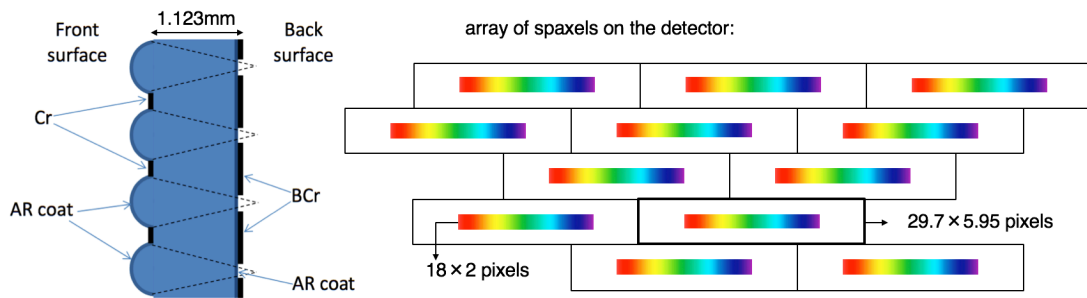

Figure 4. Left: cross section of the IFS lenslet array, with pinholes etched on the back surface. Right: diagram of the array of spaxels on the detector.

Spectrograph optics

The IFS is designed to operate at 600–720nm. After the lenslet array, the light is dispersed by one prism (in the current baseline case) or by two prisms (in the forthcoming optimal case) located in collimated space between two Hastings triplet achromatic lenses, before being reimaged onto the detector. The current prism design, made of one single commercial off-the-shelf (COTS) element, will shortly be replaced by an optimized combination of two elements, to maintain the desired spectral resolution of 50 over the whole bandwidth. In the current configuration R = 45–60 over the whole band, as shown in Fig. 5.
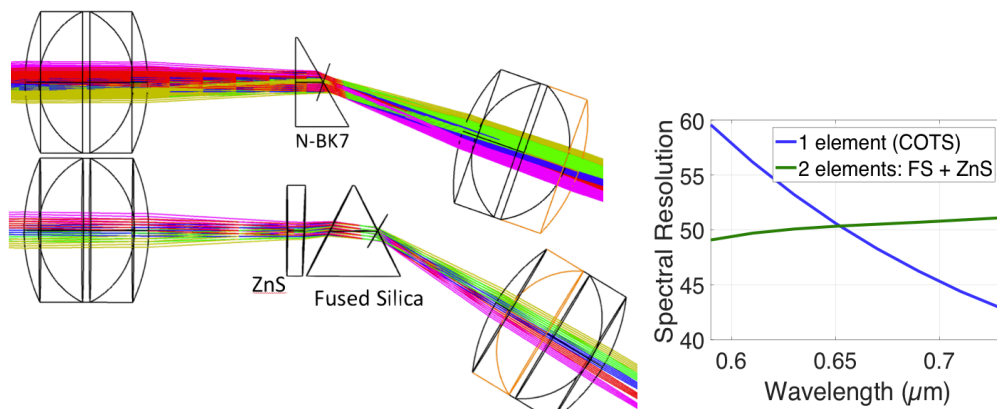
Figure 5. Left: Two envisaged options of spectrograph optics. Right: Comparison of the spectral resolution of the two options.
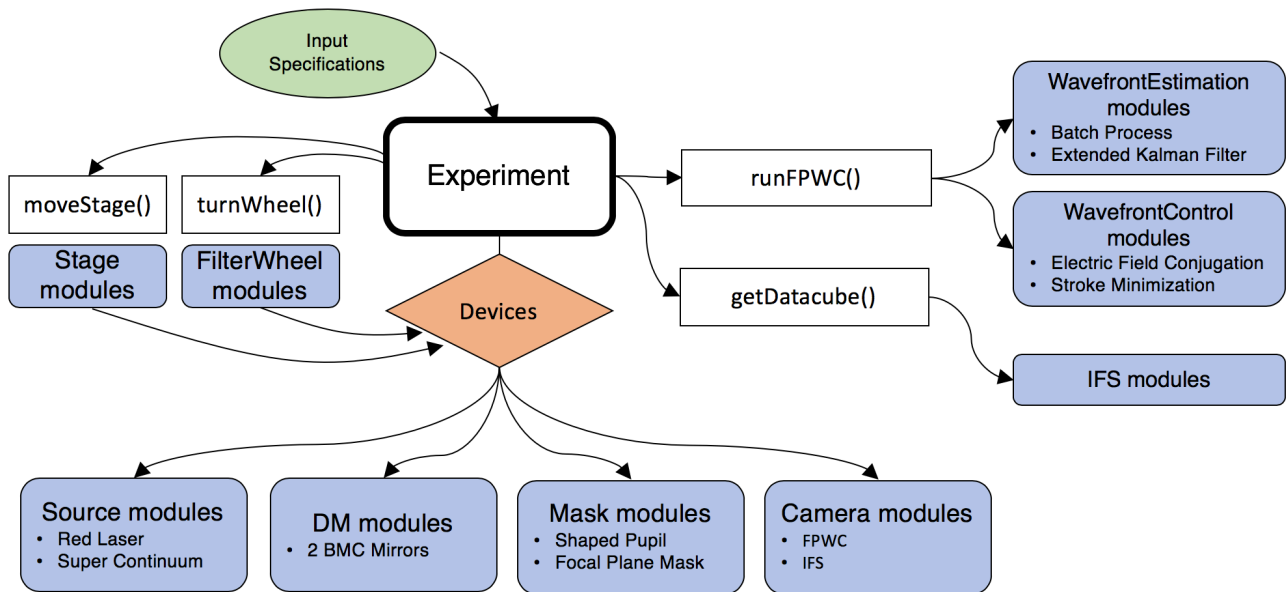
Figure 6. A flow chart describing the High Contrast Integral Field Spectrograph (HCIFS) software. The main object is an instance of the Experiment class, which receives all user input specifications through a JSON script file, represented here by the green oval. The blue rectangles are modules. All the device modules are grouped in a list represented here by the red diamond. The other white boxes are the principal methods of the main Experiment class.

3.2 The HCIFS software

The High Contrast Integral Field Spectrograph (HCIFS) software is developed using Python. It can be found on GitHub at https://github.com/ChrisDelaX/HCIFS. When using the software, an Experiment object is first constructed with a JSON script file as an argument. The script contains the input specifications and can be easily changed to allow different modules and settings to be used. A dictionary containing the module names for each device used in the lab setup is included in the JSON script. The Experiment object uses this dictionary to load a list of Device instances corresponding to hardware components present in the lab. The principal methods of the Experiment object are the following:

- **turnWheel() and moveStage()**: Two high-level methods allow controlling filter wheels and motorized stages in order to modify certain devices (e.g., the source wavelength), or move them (e.g., the focal plane mask, the camera). Moving an individual component simultaneously updates the relative distances between the adjacent devices.

- **runFPWC()**: This method performs an FPWC experiment, using one of the two operation modes of the lab: the imaging mode with the QSI camera, or the spectroscopy mode with the Starlight Xpress camera located in the IFS. Currently, only the imaging mode can be operated in closed loop to reach a high contrast level in monochromatic light, as presented in the previous section. The spectroscopy mode is operational in open loop, but more developments are necessary to allow the automation of the wavefront control in closed loop with the IFS camera.

- **getDatacube()**: When operating the lab in broadband, this method is intended to function as a pipeline to process images from the IFS by importing and calling open-source Python packages such as CRISPY[16] (see https://github.com/mjrfringes/crispy for more detail). Our pipeline is still under construction. The ultimate goal is to allow the user to reconstruct 3D datacubes from IFS spatio-spectral science images.

3.3 First light results

In its current state, the HCIFS does not allow controlling the DMs in spectroscopy mode. This feature will be added shortly to our control software. In the meantime, dark holes can still be created in the IFS by running FPWC in imaging mode, then switching to the spectroscopy mode with the addition of a pickoff flat mirror. Using this method, we have been able to perform preliminary tests on the IFS. Such an operation naturally introduces non-common path aberrations. It also does not allow the FPWC to remain active while operating the IFS, so the performance in the IFS degrades slowly with time. Nevertheless, we successfully managed to produce our first light result with the IFS in broadband as illustrated in Fig 7. After setting the focal plane mask to its on-axis position, we measured a contrast value of $\sim 10^{-5}$ in the dark holes. The spectra length and spacing values are about 10% larger than our design specifications. This is mainly due to misalignments in our temporary spectrograph optics design, and it should be improved in our forthcoming optimal design.
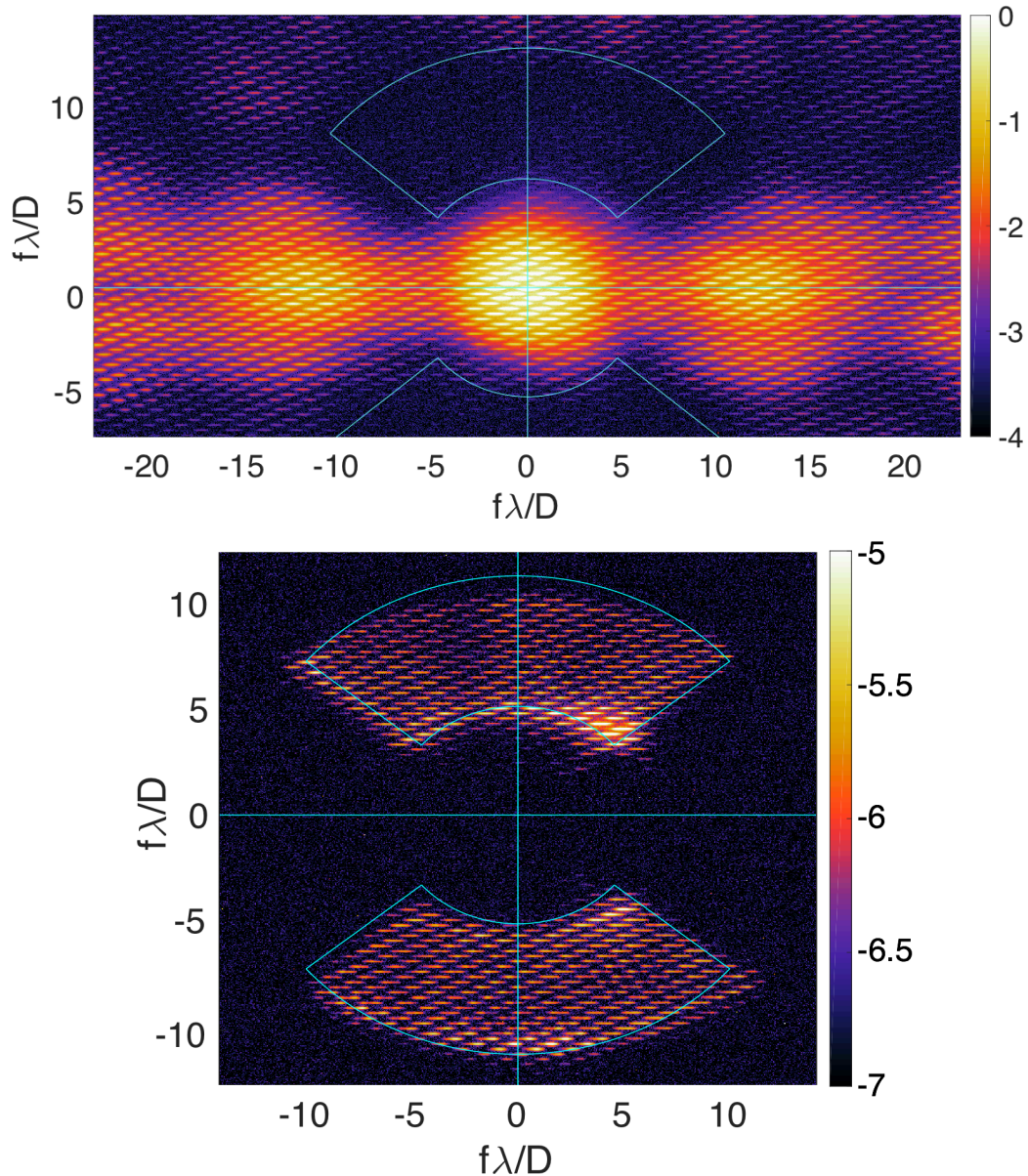
Figure 7. First light of the IFS in broadband. Two dark holes were formed with closed-loop FPWC in imaging mode, then the spectroscopy mode was enabled by switching to a broadband source. Top: Focal plane mask is off-axis. Bottom: Focal plane mask is on-axis, and the contrast in the dark holes is about 10^{-5}.

4. CONCLUSIONS

We provide an update on the ongoing development of a High Contrast Integral Field Spectrograph (HCIFS) at Princeton University. We give a detailed description of the lenslet array-based HCIFS layout and its optical design. The current design is only temporary. An improved design with better prisms is to be installed in the coming weeks, and it is expected to allow a more constant spectral resolution over the 18% bandwidth. First light in open loop was obtained, and it shows encouraging results with broadband contrast of 10^{-5}. The HCIFS Python software is now operational, and the next step is to integrate the data reduction pipeline using the CRISPY Python package to generate IFS data cubes.

REFERENCES

[1] B. Macintosh, J. R. Graham, P. Ingraham, et al., "First light of the Gemini Planet Imager," Proc Natl Acad Sci U S A **111(35)**, 12661–12666 (2014).

[2] M. C. Noecker, F. Zhao, R. Demers, et al., "Coronagraph instrument for wfirst-afta," JATIS **2(1)**, 011001 (2016).

[3] M. W. McElwain, A. M. Mandell, Q. Gong, et al., "PISCES: an integral field spectrograph technology demonstration for the WFIRST coronagraph," Proc. SPIE **99041A**, 99041A18 (2016).

[4] H. Sun, N. J. Kasdin, R., Vanderbei, et al., "Improved high-contrast wavefront controllers for exoplanet coronagraphic imaging systems," Proc. SPIE **10400**, 104000R (2017).

[5] H. Sun, N. J. Kasdin, R., Vanderbei, "Identification of the focal plane wavefront control system using E-M algorithm," Proc. SPIE **10400**, 1040028 (2017).

[6] N. J. Kasdin et al., "Extrasolar planet finding via optimal apodized-pupil and shaped-pupil coronagraphs, " Astrophys. J. **582**(1), 1147–1161 (2003).

[7] N. J. Kasdin, R., Vanderbei, M. Littman, et al., "The shaped pupil coronagraph for planet finding coronagraphy: optimization, sensitivity, and laboratory testing," Proc. SPIE **5487**, 1312 (2004).

[8] R. Belikov et al., "Demonstration of high contrast in 10% broadband light with the shaped pupil coronagraph," Proc. SPIE **6693**, 66930Y (2007).

[9] L. Pueyo et al., "Optimal dark hole generation via two deformable mirrors with stroke minimization," Appl. Opt. **48**(32), 6296–6312 (2009).

[10] R. Belikov et al., "Laboratory demonstration of high-contrast imaging at inner working angles 2 λ/D and better," Proc. SPIE **8151**, 815102 (2011).

[11] T. D. Groff et al., "Broadband focal plane wavefront control of ampli- tude and phase aberrations," Proc. SPIE, **8442**, 84420C (2012).

[12] T. D. Groff and N. J. Kasdin, "Kalman filtering techniques for focal plane electric field estimation," JOSA A **30(1),** 128–139 (2013).

[13] A. Riggs et al., "Demonstration of symmetric dark holes using two deformable mirrors at the high-contrast imaging testbed," Proc. SPIE **8864**, 88640T (2013).

[14] A. Riggs, N. J. Kasdin, and T. D. Groff, "Recursive starlight and bias estimation for high-contrast imaging with an extended Kalman filter," JATIS **2(1),** 011017 (2016).

[15] T. D. Groff, A. E. Riggs, B. Kern, and N. J. Kasdin, "Methods and limitations of focal plane sensing, estimation, and control in high-contrast imaging," JATIS **2(1),** 011009 (2016).

[16] M. J. Rizzo, T. D. Groff, N. T. Zimmerman, et al., "Simulating the WFIRST coronagraph Integral Field Spectrograph," Proc. SPIE **10400**, 104000B (2017).